

Direct Deposit Laminate Nanocomposites with Enhanced Propellant Properties

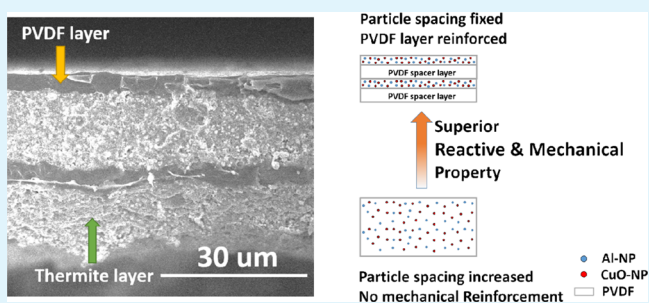
Xiangyu Li,[†] Philip Guerieri,[‡] Wenbo Zhou,[‡] Chuan Huang,[†] and Michael R. Zachariah*[†]

Department of Chemical and Biomolecular Engineering and Department of Chemistry and Biochemistry, University of Maryland, College Park, Maryland 20742, United States

Supporting Information

ABSTRACT: One of the challenges in the use of energetic nanoparticles within a polymer matrix for propellant applications is obtaining high particle loading (high energy density) while maintaining mechanical integrity and reactivity. In this study, we explore a new strategy that utilizes laminate structures. Here, a laminate of alternating layers of aluminum nanoparticle (Al-NPs)/copper oxide nanoparticle (CuO-NPs) thermites in a polyvinylidene fluoride (PVDF) reactive binder, with a spacer layer of PVDF was fabricated by an electrospray layer-by-layer deposition method. The deposited layers containing up to 60 wt % Al-NPs/CuO-NPs thermite are found to be uniform and mechanically flexible. Both the reactive and mechanical properties of laminate significantly outperformed the single-layer structure with the same material composition. These results suggest that deploying a multilayer laminate structure enables the incorporation of high loadings of energetic materials and, in some cases, enhances the reactive properties over the corresponding homogeneous structure. These results imply that an additive manufacturing approach may yield significant advantages in developing a tailored architecture for advanced propulsion systems.

KEYWORDS: nanocomposite, propellant, laminate, thermite, mechanical property, polymer, print



1. INTRODUCTION

Micron scale metal particles such as aluminum have been traditionally used as an important component in solid rocket propellants due to its high energy density and high energy release rate during oxidation. On the other hand, the use of nanoscale metalized propellants have failed to gain much traction, despite their lower ignition temperature and fast burn rates associated with the enhanced surface area of these materials.^{1–4} As nominally implemented, the metal and oxidizer are incorporated within a polymer binder, the purpose of which is to create a motor grain with mechanical integrity and ideally participate in a favorable manner in the overall energy release chemistry.^{5–7} A variety of binders have been employed including epoxy, nitrocellulose, and fluorine containing polymers.^{8–11} In the latter case, fluorine-containing binders offer a delivery method for a very strong oxidizer.^{12,13} However, while nanoscale reactive components offer high-potential game-changing performance, fabricating polymer formulations with high mass loading of these reactive components has proved to be very challenging. In part, this is due to the rapid increase in viscosity of the polymer melt upon addition of high surface area nanomaterials that makes casting virtually impossible.^{14,15} This can lead to an inhomogeneous mixture, aggregation, and poor mechanical properties. As reported in previous works,^{16,17} nanostructured materials play an important role in the mechanical properties of nanomaterial–polymer nanocomposite. Due to the formation of a co-network between the

nanomaterial and the polymer chain, nanocomposites with small nanostructured materials such as nanoparticles, nano-sheets, and nanotubes in the polymer matrix demonstrate enhanced mechanical integrity relative to the corresponding pure polymer. However, higher loadings of nanomaterial result in agglomeration and ultimately lead to significantly degraded mechanical properties.^{18,19}

One way to enhance mechanical strength is to create a laminate structure. Many properties including fracture toughness, fatigue behavior, impact behavior, wear corrosion, and damping capacity can be dramatically improved by employing a laminated structure.²⁰ In this manner, materials that may by themselves be impractical for mechanical reasons may be stabilized within such a structure.

In this work, we employ a laminate structure to enhance both the reactive and structural properties of the energetic propellant. The fuel/oxidizer solids to be explored are drawn from the class of nanothermites that are highly reactive and can lead to as much as 1000× enhancement in reactivity as compared to their micron counterparts.^{21,22}

Electro-spray or electrohydrodynamic deposition has been employed to generate solid thin films.^{23–25} In this approach, aerosol droplets can be ejected from a liquid surface by

Received: January 29, 2015

Accepted: March 27, 2015

Published: March 27, 2015

applying a high electric field to overcome the surface tension and the intermolecular forces at the solution interface. If the liquid has a dispersion of precursor materials (e.g., particles), the droplets generated will contain the additive. Because the dominant force for atomization is electrostatic, the drops generated will typically undergo Coulombic explosion via a “droplet fission” process, which typically leads to a very narrow drop size distribution, unable to be obtained by other spray methods.²⁶ By tuning the solution electrical conductivity and surface tension, the drop size can be manipulated.^{27–31} Further, because the droplets are charged, they can be easily directed to a substrate to create a film. To create the laminate structure, we build on prior work in the use of electro-spray deposition as a simple method to fabricate nanocomposites with high nanoparticle loadings.³² The laminate is composed of alternating layers of Al-NPs/CuO-NPs thermites in a PVDF reactive binder, with a spacer layer of PVDF. These results show that enhancement in both the reactive and mechanical property are found in laminate films.

2. MATERIALS AND METHODS

2.1. Materials. Aluminum nanopowders (Al-NPs; ALEX, 50 nm) were purchased from Argonide Corporation and tested by thermogravimetric methods to determine the active Al content as ~70% by mass.^{9,32,34,35} Polyvinylidene fluoride (PVDF; $M_w = 534,000$), dimethylformamide (DMF; 99.8 wt %), copper oxide nanopowders (CuO-NPs; 99.8 wt %, ~30 nm), and ammonium perchlorate (AP; 99.8 wt %) were purchased from Sigma-Aldrich.

2.2. Precursor Preparation. For a typical fabricating process, (a laminate Al/CuO thermite–PVDF film), 400 mg of PVDF was dissolved in 6 mL of DMF to create the precursor for the PVDF layer. The precursor used to form the Al/CuO thermite layer in double layer and laminate films included 300 mg of PVDF dissolved in 6 mL of DMF, followed by dispersing 408 mg of Al-NPs, 531 mg of CuO-NPs into the prepared PVDF/DMF solution. In addition, we found that a small quantity 18 mg of AP was useful in stabilizing the electro-spray to create a crack-free thermite layer. The mixture was stirred vigorously for 30 min and ultrasonically mixed for 60 min to allow the nanoparticles to disperse homogeneously. This was followed by an additional 24 h of magnetic stirring at room temperature.

2.3. Electro-spray Deposition. As presented in Figure 1, electro-spray of pure PVDF and the thermite mixture could be alternated by the use of a dual spray setup. For this work, we employed 0.023 mm inner diameter stainless tubing for the electro-spray injector which were fed by a syringe pump operating at 2 mL hr⁻¹. A rotating

collector held at a ground potential was used to collect the laminate film. The jet-to-substrate distance was held at 6 cm and was chosen empirically so as to enable a wide spray pattern, and sufficient time was given to evaporate the solvent so as not to have visible pooling of liquid on the substrate. A linear field strength operated in the range of ~2–3 kV cm⁻¹ resulted in a stable cone-jet mode and was the nominal operating condition. The thickness of each layer can be easily adjusted by the duration of the electro-spray deposition.

2.4. Characterization. The reactive behavior of the thermite laminate film was characterized using a homemade combustion test setup. The prepared films had sufficient mechanical strength to be easily removed from the substrate backing; they were cut into 2.5 × 0.5 cm sections and placed inside a transparent chamber filled with ambient argon. All samples were ignited at one end by resistively heating a Ni–Cr wire triggered by an external DC power supply. A high-speed camera (Phantom v12.0) with a frame rate of 7000 frames per second was deployed to record the combustion process. The videos generated from the camera was analyzed by PCC 1.2 software (Phantom, Inc.; Figure S1, Supporting Information).

Scanning electron microscopy (SEM, Hitachi, SU-70 FEG-SEM) equipped with energy dispersive X-ray spectroscopy (EDS) was used to characterize the morphologies and thickness of the laminate film. The film was cut into narrow strips (~1 mm width) and then fractured in liquid nitrogen to obtain a flat and uniform fracture section for the cross-sectional image. All samples were sputter coated with carbon prior to imaging.

The mechanical properties of the laminate film were obtained by a homemade microtensile tester.³³ Three strip specimens (2.5 cm × 0.5 cm) were tested for each film. The quasi-static loading strain rate of 10⁻⁴ s⁻¹ was applied by a customized picomotor control software. A video extensometer was used to acquire strain data in the gage section of the specimen. The load data from the load cell was obtained with Correlated Solutions (Columbia, SC) Vic-Gauge 2006 software. Before the test, the initial thickness was obtained by SEM, and the width of the film was carefully measured using a digital caliper.

3. RESULTS AND DISCUSSION

3.1. Morphology Characteristics. Figure 2 shows SEM and EDS images of the deposited films. The standalone PVDF film, (Figure 2a,b) shows a crack free, smooth and uniform polymer film. However, the standalone Al/CuO/PVDF thermite layer film (Figure 2c), as would be expected, shows a much rougher fracture surface but still maintained a uniform thickness. Under high magnification (Figure 2d), one can see that the PVDF is forming a fibrous polymer network connecting and enveloping the nanoparticles. EDS mapping (Figure 2g–j) indicates that some aggregation of the nanoparticles occurs. Finally, we can see that alternating the spray precursors leads to a well-defined laminate film (Figure 2e), with considerable lateral conformity and thickness, and the layers appears to be conformal at the interfaces (Figure 2f). We find no clear difference in morphology between the laminate structure and the standalone films.

3.2. Reactive Properties. To compare the reactive properties for both single and layer films, we prepared single- and double-layer films of the same total composition but with a different spatial arrangement. First, the double-layer films, which are composed of one layer of PVDF and one layer of thermite, were fabricated with fixed thermite layer thickness (10 μm) but different PVDF layer thicknesses. In all cases, the component concentrations in the thermite were held at 24 wt % PVDF, 33 wt % Al, and 43 wt % CuO in the thermite layer. The 24 wt % of PVDF was carefully chosen to obtain a high particle loading film as well as sufficient mechanical strength to be handled easily without breaking. Ranging from 0 to 87 wt % the mass ratio of PVDF in the whole film is increasing while the

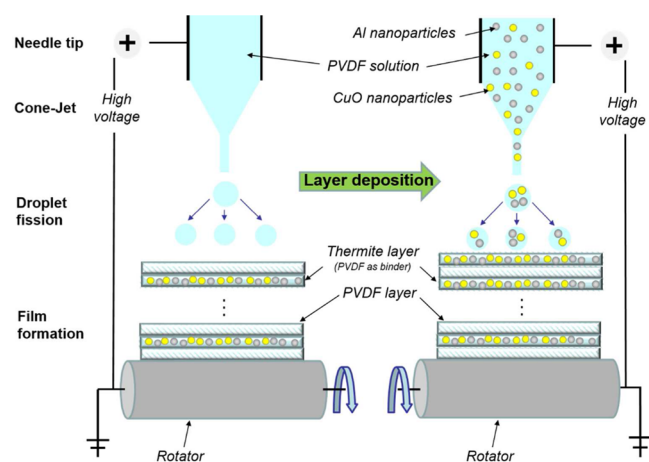


Figure 1. Illustration of electro-spray deposition process for fabricating laminate Al/CuO/PVDF thermite–PVDF films.

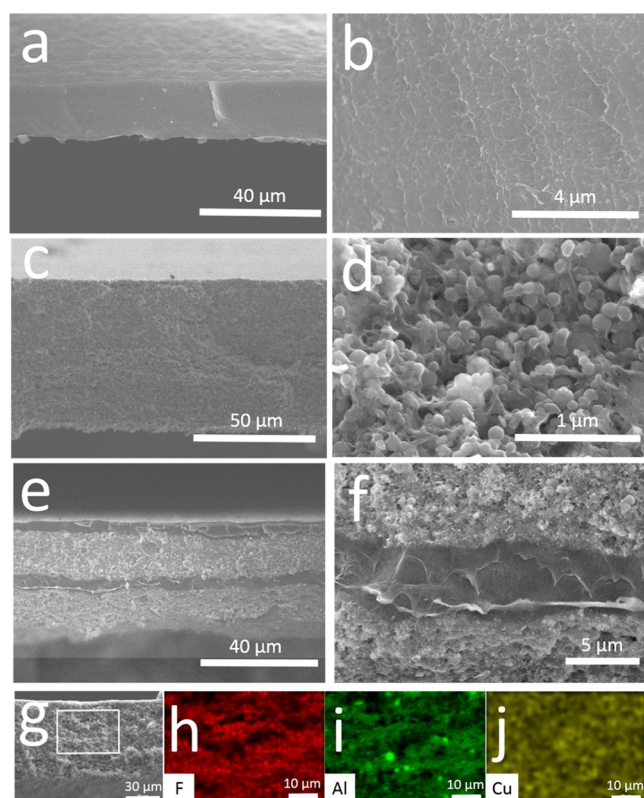
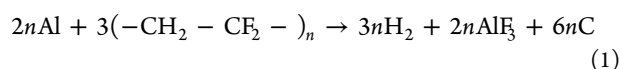


Figure 2. Cross-sectional SEM images of (a and b) PVDF film, (c and d) Al/CuO/PVDF thermite film, (e) four-layer laminate film, and (f) interfacial area. (g–j) EDS image of Al/CuO/PVDF thermite film.

PVDF layer became thicker. The combustion propagation velocity was measured by igniting a 2.5 cm length by 0.5 cm width film in ambient argon. The length of the sample was carefully measured by a digital caliper before each test. The time of the combustion propagation process was considered to be the time between the first and last spark appeared in the videos recorded by the high speed camera. For each sample, three experiments were run to calculate the average combustion propagation velocity.

In our prior work we proposed the following global reactions³²



According to eqs 1 and 2, the thermite layer as presented is with a molar ratio of PVDF/Al/CuO = 0.5/1.1/0.7, corresponding to a fuel rich layer (stoichiometry for complete reaction: molar ratio of PVDF/Al/CuO is 1.0/1.1/0.7), as will be discussed later. As such, in this experiment, the thermite layer always has the same solids loading. For each double-layer film, a single-layer film with same composition was also prepared. The thermite layer thickness, PVDF layer thickness, PVDF mass ratio, and stoichiometry of the whole film of double and single layer films are summarized in Table 1.

All the films above could be ignited easily and showed a self-sustaining stable propagating combustion except for the single-layer film with 87 wt % PVDF. Figure 3 shows the average combustion propagation velocity of the double layer, and corresponding single layer films with different PVDF mass ratio in argon, and clearly indicating that under all conditions the

Table 1. Thermite and PVDF Layer Thickness, PVDF Mass Ratio and Stoichiometry of the Whole Film of Double and Single Layer Films

double-layer film			
PVDF mass ratio (%)	molar ratio PVDF/Al/CuO	thermite layer thickness (μm)	PVDF layer thickness (μm)
24	0.5/1.1/0.7	10	0
38	1.0/1.1/0.7	10	2.5
51	1.6/1.1/0.7	10	5
76	2.8/1.1/0.7	10	20
87	10.5/1.1/0.7	10	45
single-layer film			
PVDF mass ratio (%)	molar ratio PVDF/Al/CuO		
24	0.5/1.1/0.7		
38	1.0/1.1/0.7		
51	1.6/1.1/0.7		
76	2.8/1.1/0.7		
87	10.5/1.1/0.7		

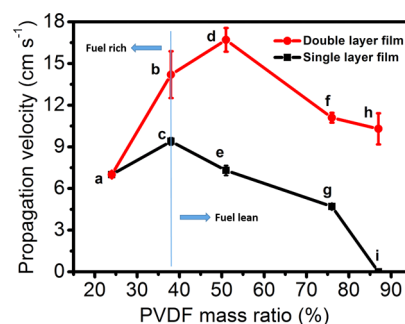


Figure 3. Average propagation velocity of double-layer (points a, b, d, f, h) and single-layer (points a, c, e, g, and i) thermite films as a function of PVDF mass ratio, when the thermite layer thickness is fixed at 10 μm in double layer thermite film. Particle concentration in thermite layer is fixed in double layer thermite films.

double layer films are superior. The left most data point (point a) corresponding to zero PVDF layer thickness, is actually just a single layer film. Both types of films follow the same basic trend. For double layer films, the combustion propagation velocity of sample with 51 wt % (Point d) PVDF is higher than films with other PVDF concentration. As for the corresponding single layer ones, the 38 wt % (point c) case had the fastest propagation velocity. At a PVDF mass ratio of 87 wt %, the bottom most portion of the PVDF layer in the double layer film (point h) was unburned while the corresponding single layer film (point i) was unable to burn at all.

For both single- and double-layer films, the molar ratio of PVDF is increasing from point a to points h and i. The stoichiometric composition (PVDF mass ratio 38 wt %), point c (becomes lean with increasing PVDF) shows the fastest propagation velocity in argon for the single layer films.

For the double-layer, the fastest propagation velocity occurs at a PVDF mass ratio of 51 wt % (point d), and thus is stoichiometrically fuel lean. This can be understood as requiring extra oxidizer over stoichiometric because of the spatial separation in the two layer film, relative to the single layer case. A possible mechanism of the reactive behavior could be that when the PVDF is below 51 wt %, the combustion propagation velocity is decreasing due to the lack of PVDF to enhance all of the thermite layer. Above 51 wt %, not all of the thermite layer can be enhanced due to the decomposition of

Table 2. Number of Layers, Thermite Layer Thickness, PVDF Layer Thickness, and Total Film Thickness of Sample Groups 1 and 2

group	no. of layers	thermite layer thickness (μm)	PVDF layer thickness (μm)	total film thickness (μm)
group 1	2	30	7	37
	4	30	7	74
	6	30	7	111
group 2	2	90	21	111
	4	45	10.5	111
	6	30	7	111

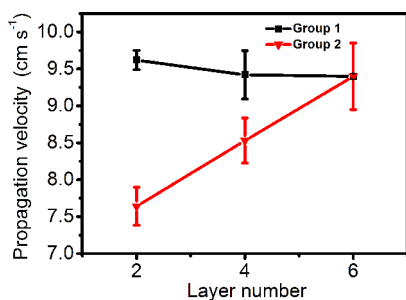


Figure 4. Average combustion propagation velocity of laminate film sample groups 1 and 2. In group 1, all the PVDF layers were fixed at $7\ \mu\text{m}$, and the thermite layers were fixed at $30\ \mu\text{m}$. In group 2, the thickness ratio of the thermite layer and the PVDF spacer layer is 30/7 in each laminate film with the same total film thickness of $111\ \mu\text{m}$, and thus, as we increase the number of layers, the absolute layer thickness decreases.

unreacted PVDF, which acts as a heat sink. In fact, at point h, the thermite cannot support complete combustion and an unburned PVDF layer remains. Importantly, however, all double-layer films demonstrate a higher combustion propagation velocity than the corresponding single layer film.

It is well accepted that the interfacial contact between the fuel and oxidizer plays an important role in the combustion performance of composite energetic materials such as nanothermites.^{34,35} In this case, although the double- and corresponding single-layer films have the same material

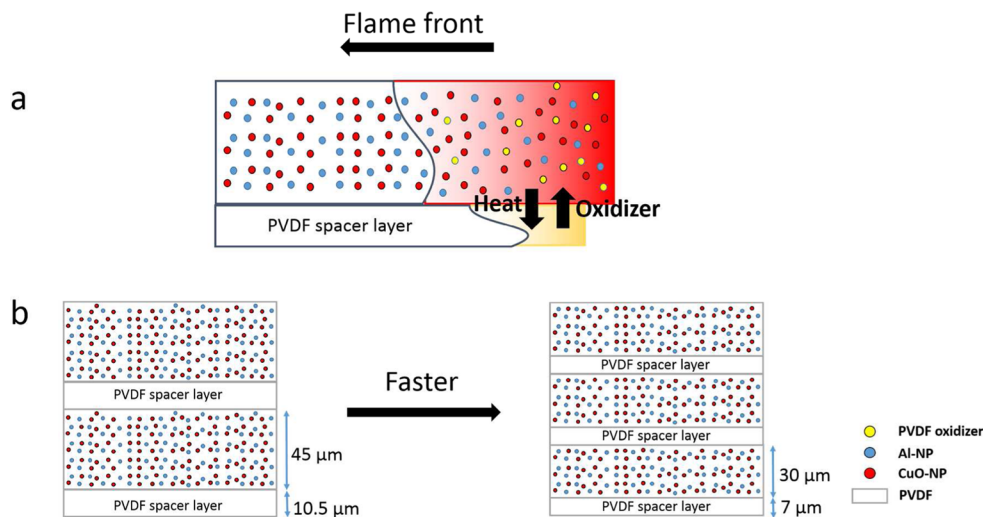


Figure 5. (a) Conceptual model of the reaction mechanism between the thermite layer and PVDF layer of 2 layers laminate film. (b) Decreasing the spacing between the thermite and PVDF layers enhances the propagation speed of the film.

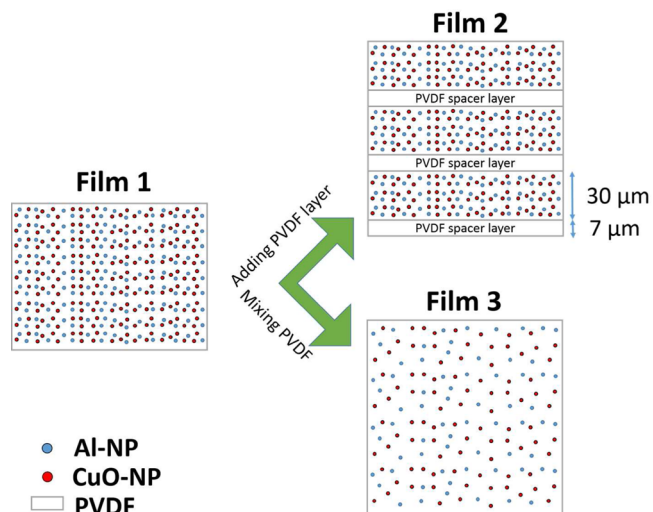


Figure 6. Film 1: thermite/PVDF. Film 2: film 1 with additional PVDF spacer layers to create a six-layer film. Film 3: film 2 but with the thermite particles dispersed evenly.

composition, the interparticle distance between fuel and oxidizer are different, and in particular, it is the single-layer film with the greater distance (Figure S2, Supporting Information). Thus, by partitioning the thermite within a concentrated region, we can keep the same equivalence ratio, and enhance the burning rate. The reason for not simply concentrating particles in a single layer will become apparent when we discuss mechanical properties.

The reactive properties of multilayer films are investigated because they are ultimately how a formulated propellant could be built up. PVDF layers and thermite layers were deposited alternately in all laminate films. Thermite layers in the laminate films contain 24 wt % PVDF, 33 wt % Al, and 43 wt % CuO, as above. Two groups of samples consisting of 2, 4, and 6 layers were prepared. In group 1, all the PVDF spacer layers were fixed at $7\ \mu\text{m}$, and the thermite layers were fixed at $30\ \mu\text{m}$. In group 2 the thickness ratio of thermite layer and PVDF spacer layer were fixed at 30/7 in each laminate film, with the same total film thickness of $111\ \mu\text{m}$; thus, as we increase the number

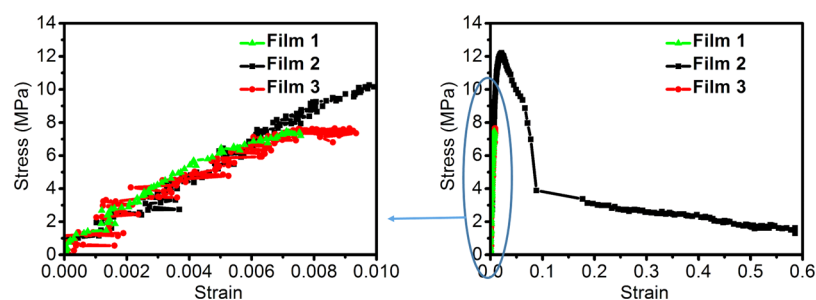


Figure 7. Stress–strain curves of (green) film 1, (black) film 2, and (red) film 3. Film 1: Thermite/PVDF. Film 2: film 1 with additional PVDF spacer layers to create a six-layer film. Film 3: film 2 but with the thermite particles dispersed evenly.

of layers, the absolute layer thickness decreases (unlike group 1). All samples in the two groups have the same total material composition of 39 wt % PVDF, 26 wt % Al, and 35 wt % CuO because they have the same thermite/PVDF layer thickness ratio. The laminate films with six layers in both groups actually have the same overall composition. The specific parameters of the samples are listed in Table 2. Figure 4 demonstrates the combustion propagation velocity of the two groups of samples. For group 1, the combustion propagation velocity of the films shows no obvious difference, with an increase in number of layers. This is not surprising, as we should not expect any significant cooperative effect of stacking multiple layers. It also implies that a large structure on the length scale of a rocket motor could be fabricated using this approach. On the other hand, group 2, which consists of laminates with a fixed total thickness, clearly shows propagation velocity enhancement as the bilayer spacing is decreased.

Figures 3 and 4 imply that the length scale of particle separation is not the only relevant scale. Keep in mind that all these structures are globally stoichiometric. However, as we saw in Figure 3, the burn rate was enhanced in a two-layer structure. Thus, the adjacent PVDF layer has a role to play in enhancing the burn rate. Our conceptual model to explain the observation that decreasing the layer thickness enhances the reaction velocity may be considered in the following way (Figure 5). The thermite layer will obviously, on its own, have a faster propagation velocity than the PVDF spacer layer. As such, one can imagine that the spacer layer erosion rate will lag behind due to the heat flux, q , needed to decompose and release this layer. Because the thermite layer is fuel-rich, as the PVDF layer is heated, it can participate in the reaction by transporting oxidizer, m , into the postreaction region (Figure 5a). Decreasing the spacing decreases the effective path length for transport of oxidizer species to complete the reaction and thus enhances the propagation speed (Figure 5b). By decreasing the spacing therefore between the thermite and PVDF layer, we expect to see enhanced propagation as shown in group 2 in Figure 4.

3.3. Mechanical Performance. A major reason to explore the use of laminates is to improve the mechanical properties of heavily particle loaded polymer. To evaluate the potential advantages of laminate structures, three different films were constructed (Figure 6).

Figure 7 shows the stress–strain behavior of the three structures, and demonstrates that the laminate (film 2) greatly outperformed the same structure without the spacer layer (film 1). The tensile strength of the laminate showed a $\sim 62\%$ improvement over both the corresponding single layer and the dispersed particle layer (film 3). The laminate has a strain of

58%, which is considerably better than the corresponding 0.91% for the dispersed structure of film 3, and dropped to 0.76% for the thermite/PVDF film 1. Similarly, the toughness of the laminate is 5 times higher than film 3, and 38 times larger than film 1 (Table S1, Supporting Information). Also, the mechanical property of the laminate is considerably better than single layer PVDF/Al-NPs energetic nanocomposite with similar material composition³² (Table S2, Supporting Information). Thus, we can conclude that a laminate structure greatly improves the mechanical properties of high loading particle systems. When a load is applied on a laminated composite, part of the load on the matrix is transferred onto the reinforcement through the interface. In our case, the mechanical behavior of the pure PVDF spacer layer is superior to the thermite layers with a tensile strength of 18 MPa, strain of 110%, and toughness of 19 MJ m^{-3} ,³² and thus, it acts as a reinforcement for the thermite layer matrix in the composite. The load applied on the weak thermite matrix is partially transferred onto the strong PVDF reinforcement through the interfacial area.

4. CONCLUSION

A direct deposition process is demonstrated to create laminate nanothermite-based energetic polymer films. These structures show enhanced performance, with combustion propagation velocity correlated with decreasing layer separation. The mechanical properties of laminate films are far superior to single-layer films, including similar films in our earlier work and demonstrate that high metal loadings can be achieved using this laminate structure. This result suggests that layered structures may offer significant advantages in the formation of large propellant structures. Moreover, this direct deposition technique could find application for the creation of nanoparticle-catalyst materials for other propulsion/catalyst applications.^{36–38}

■ ASSOCIATED CONTENT

Supporting Information

Additional specific parameters of double and corresponding single layer film, conceptual explanation of the difference of particle distance in double and corresponding single layer films, and illustrations of the three samples in the mechanical test. This material is available free of charge via the Internet at <http://pubs.acs.org>.

■ AUTHOR INFORMATION

Corresponding Author

*E-mail: mrz@umd.edu. Phone: +001 301-405-4311. Fax: +001 301-314-947.

Present Address

[†]X.L. and C.H. are currently at Nanjing University of Science and Technology, Nanjing, China

Author Contributions

[‡]The manuscript was written through contributions of all authors. All authors have given approval to the final version of the manuscript. These authors contributed equally.

Notes

The authors declare no competing financial interest.

ACKNOWLEDGMENTS

This work was supported by the Defense Threat Reduction Agency and AFOSR-MURI. We acknowledge the support of the Maryland Nanocenter and its NispLab. The NispLab is supported in part by the NSF as a MRSEC Shared Experimental Facility. X.L. is grateful for the financial support from Nanjing University of Science and Technology.

REFERENCES

- (1) Sullivan, K.; Young, G.; Zachariah, M. R. Enhanced Reactivity of nano-B/Al/CuO MIC's. *Combust. Flame* **2009**, *156*, 302–309.
- (2) Yetter, R. A.; Risha, G. A.; Son, S. F. Metal Particle Combustion and Nanotechnology. *Proc. Combust. Inst.* **2009**, *32*, 1819–1838.
- (3) Meda, L.; Marra, G.; Galfetti, L.; Severini, F.; De Luca, L. Nano-aluminum as Energetic Material for Rocket Propellants. *Mater. Sci. Eng., C* **2007**, *27*, 1393–1396.
- (4) Jian, G.; Feng, J.; Jacob, R. J.; Egan, G. C.; Zachariah, M. R. Super-reactive Nanoenergetic Gas Generators Based on Periodate Salts. *Angew. Chem., Int. Ed.* **2013**, *52*, 9743–9746.
- (5) Sadeghipour, S.; Ghaderian, J.; Wahid, M. Advances in Aluminum Powder Usage as an Energetic Material and Applications for Rocket Propellant. In Proceedings of the 4th International Meeting of Advances in Thermalfluids (IMAT 2011), Meleka, Malaysia, October 3–4, 2011; American Institute of Physics: College Park, MD, 2012.
- (6) Arkhipov, V. A.; Korotkikh, A. G. The Influence of Aluminum Powder Dispersion on Composite Solid Propellants Ignitability by Laser Radiation. *Combust. Flame* **2012**, *159*, 409–415.
- (7) Gromov, A. A.; Teipel, U. In *Metal Nanopowders: Production, Characterization, and Energetic Applications*; Wiley-VCH Verlag: Weinheim, Germany, 2014; Chapter 4, pp 79–104.
- (8) Parthiban, S.; Jain, S. R.; Rangunandan, B. Interpenetrating Polymer Networks as Binders for Solid Composite Propellants. *Def. Sci. J.* **2013**, *42*, 147–156.
- (9) Yan, S.; Jian, G.; Zachariah, M. R. Electrospun Nanofiber-based Thermite Textiles and their Reactive Properties. *ACS Appl. Mater. Interfaces* **2012**, *4*, 6432–6435.
- (10) Li, X.; Liu, X.; Cheng, Y.; Li, Y.; Mei, X. Thermal Decomposition Properties of Double-base Propellant and Ammonium Perchlorate. *J. Therm. Anal. Calorim.* **2014**, *115*, 887–894.
- (11) Miller, H. A.; Kusel, B. S.; Danielson, S. T.; Neat, J. W.; Avjian, E. K.; Pierson, S. N.; Budy, S. M.; Ball, D. W.; Iacono, S. T.; Kettwich, S. C. Metastable Nanostructured Metallized Fluoropolymer Composites for Energetics. *J. Mater. Chem. A* **2013**, *1*, 7050–7058.
- (12) Koch, E. C.. In *Metal-Fluorocarbon Based Energetic Materials*; John Wiley & Sons: Brussels, Belgium, 2012.
- (13) Smith, D. W.; Iacono, S. T.; Boday, D. J.; Kettwich, S. C. In *Advances in Fluorine-Containing Polymers*; American Chemical Society: Dayton, OH, 2012; Chapter 9, pp 127–140.
- (14) Meda, L.; Marra, G.; Galfetti, L.; Inchingalo, S.; Severini, F.; De Luca, L. Nano-composites for Rocket Solid Propellants. *Compos. Sci. Technol.* **2005**, *65*, 769–773.
- (15) Galfetti, L.; De Luca, L.; Severini, F.; Meda, L.; Marra, G.; Marchetti, M.; Regi, M.; Bellucci, S. Nanoparticles for Solid Rocket Propulsion. *J. Phys.: Condens. Matter* **2006**, *18*, S1991–S2005.
- (16) Kumar, G. V.; Rao, C.; Selvaraj, N. Mechanical and Tribological Behavior of Particulate Reinforced Aluminum Metal Matrix

Composites—A Review. *J. Miner. Mater. Charact. Eng.* **2011**, *10*, 59–91.

(17) Al-Saleh, M. H.; Sundararaj, U. Review of the Mechanical Properties of Carbon Nanofiber/Polymer Composites. *Composites, Part A* **2011**, *42*, 2126–2142.

(18) Sekitani, T.; Noguchi, Y.; Hata, K.; Fukushima, T.; Aida, T.; Someya, T. A Rubberlike Stretchable Active Matrix Using Elastic Conductors. *Science* **2008**, *321*, 1468–1472.

(19) Zuiderduin, W.; Westzaan, C.; Huetink, J.; Gaymans, R. Toughening of Polypropylene with Calcium Carbonate Particles. *Polymer* **2003**, *44*, 261–275.

(20) Chan, H. M. Layered Ceramics: Processing and Mechanical Behavior. *Annu. Rev. Mater. Sci.* **1997**, *27*, 249–282.

(21) Piercey, D. G.; Klapoetke, T. M. Nanoscale Aluminum–Metal Oxide (Thermite) Reactions for Application in Energetic Materials. *Cent. Eur. J. Energ. Mater.* **2010**, *7*, 115–129.

(22) Dreizin, E. L. Metal-based Reactive Nanomaterials. *Prog. Energy Combust. Sci.* **2009**, *35*, 141–167.

(23) Jaworek, A. Electro spray Droplet Sources for Thin Film Deposition. *J. Mater. Sci.* **2007**, *42*, 266–297.

(24) Rietveld, I. B.; Sugauma, N.; Kobayashi, K.; Yamada, H.; Matsushige, K. Electro spray Deposition of Photoresist: A Low Impact Method for the Fabrication of Multilayered Films. *Macromol. Mater. Eng.* **2008**, *293*, 387–399.

(25) Rietveld, I. B.; Kobayashi, K.; Yamada, H.; Matsushige, K. Process Parameters for Fast Production of Ultra-thin Polymer Film with Electro spray Deposition Under Ambient Conditions. *J. Colloid Interface Sci.* **2009**, *339*, 481–488.

(26) Bock, N.; Dargaville, T. R.; Woodruff, M. A. Electro spraying of Polymers with Therapeutic Molecules: State of the Art. *Prog. Polym. Sci.* **2012**, *37*, 1510–1551.

(27) Fernandez, J.; de la Mora, J. F.; Navascues, J.; Fernandez, F.; Rosell-Llompart, J. Generation of Submicron Monodisperse Aerosols in Electro sprays. *J. Aerosol. Sci.* **1990**, *21*, S673–S676.

(28) La Mora, D.; Fernández, J. The Effect of Charge Emission from Electrified Liquid Cones. *J. Fluid. Mech.* **1992**, *243*, S61–S74.

(29) Meesters, G.; Vercoulen, P.; Marijnissen, J.; Scarlett, B. The Current Emitted by Highly Conducting Taylor Cones. *J. Aerosol. Sci.* **1992**, *23*, 37–49.

(30) La Mora, D.; Fernandez, J. Generation of Micron-sized Droplets from the Taylor Cone. *J. Fluid. Mech.* **1994**, *260*, 155–184.

(31) Gamero-Castano, M.; Aguirre-de-Carcer, I.; De Juan, L.; de la Mora, J. F. On the Current Emitted by Taylor Cone-jets of Electrolytes in Vacuo: Implications for Liquid Metal Ion Sources. *J. Appl. Phys.* **1998**, *83*, 2428–2434.

(32) Huang, C.; Jian, G.; DeLisio, J. B.; Wang, H.; Zachariah, M. R. Electro spray Deposition of Energetic Polymer Nanocomposites with High Mass Particle Loadings: A Prelude to 3D Printing of Rocket Motors. *Adv. Eng. Mater.* **2015**, *17* (1), 95–101.

(33) Gershon, A. L.; Cole, D. P.; Kota, A. K.; Bruck, H. A. Nanomechanical Characterization of Dispersion and its Effects in Nano-enhanced Polymers and Polymer Composites. *J. Mater. Sci.* **2010**, *45*, 6353–6364.

(34) Sullivan, K. T.; Piekielek, N. W.; Wu, C.; Chowdhury, S.; Kelley, S. T.; Hufnagel, T. C.; Fezzaa, K.; Zachariah, M. R. Reactive Sintering: An Important Component in the Combustion of Nanocomposite Thermites. *Combust. Flame* **2012**, *159*, 2–15.

(35) Sullivan, K. T.; Chiou, W. A.; Fiore, R.; Zachariah, M. R. In Situ Microscopy of Rapidly Heated Nano-Al and Nano-Al/WO₃ Thermites. *Appl. Phys. Lett.* **2010**, *97*, 1331041–3.

(36) Claussen, J. C.; Daniele, M. A.; Geder, J.; Pruessner, M.; Mäkinen, A. J.; Melde, B. J.; Medintz, I. L. Platinum-Paper Micromotors: An Urchin-like Nanohybrid Catalyst for Green Monopropellant Bubble-Thrusters. *ACS Appl. Mater. Interfaces* **2014**, *20*, 17837–17847.

(37) McMahon, B. W.; Perez, J. P. L.; Yu, J.; Boatz, J. A.; Anderson, S. L. Synthesis of Nanoparticles from Malleable and Ductile Metals Using Powder-Free, Reactant-Assisted Mechanical Attrition. *ACS Appl. Mater. Interfaces* **2014**, *22*, 19579–19591.

(38) Wei, X.; Yang, X. F.; Wang, A. Q.; Li, L.; Liu, X. Y.; Zhang, T.; Mou, C. Y.; Li, J. Bimetallic Au–Pd Alloy Catalysts for N₂O Decomposition: Effects of Surface Structures on Catalytic Activity. *J. Phys. Chem. C* **2012**, *116*, 6222–6232.